

Step-like resistance changes in VO₂ thin films grown on hexagonal boron nitride with *in situ* optically observable metallic domains

Cite as: Appl. Phys. Lett. 120, 053104 (2022); <https://doi.org/10.1063/5.0072746>

Submitted: 24 September 2021 • Accepted: 11 January 2022 • Published Online: 01 February 2022

 Shingo Genchi, Mahito Yamamoto,  Takuya Iwasaki, et al.



View Online



Export Citation



CrossMark

 QBLOX



1 qubit

Shorten Setup Time

Auto-Calibration

More Qubits

Fully-integrated

Quantum Control Stacks

Ultrastable DC to 18.5 GHz

Synchronized <<1 ns

Ultralow noise



100s qubits

[visit our website >](#)

Step-like resistance changes in VO₂ thin films grown on hexagonal boron nitride with *in situ* optically observable metallic domains

Cite as: Appl. Phys. Lett. **120**, 053104 (2022); doi: [10.1063/5.0072746](https://doi.org/10.1063/5.0072746)

Submitted: 24 September 2021 · Accepted: 11 January 2022 ·

Published Online: 1 February 2022







View Online



Export Citation



CrossMark

Shingo Genchi,¹  Mahito Yamamoto,² Takuya Iwasaki,³  Shu Nakaharai,³ Kenji Watanabe,⁴  Takashi Taniguchi,³ Yutaka Wakayama,³ and Hidekazu Tanaka^{1,a)} 

AFFILIATIONS

¹SANKEN (Institute of Scientific and Industrial Research), Osaka University, 8-1 Mihogaoka, Ibaraki, Osaka 567-0047, Japan

²Faculty of Engineering Science, Kansai University, 3-3-35 Yamate-cho, Suita, Osaka 564-8680, Japan

³International Center for Materials Nanoarchitectonics, National Institute for Materials Science, 1-1 Namiki, Tsukuba, Ibaraki 305-0044, Japan

⁴Research Center for Functional Materials, National Institute for Materials Science, 1-1 Namiki, Tsukuba, Ibaraki 305-0044, Japan

^{a)} Author to whom correspondence should be addressed: h-tanaka@sanken.osaka-u.ac.jp

ABSTRACT

Vanadium dioxide (VO₂) thin films grown on hexagonal boron nitride (hBN) flakes show three orders of magnitude resistance change due to metal–insulator transition (MIT). The MIT property of VO₂ thin films is strongly dependent on the metallic domain size, which should be identified to derive the resistance change owing to the single metallic domain. In this study, we investigated the relationship between the metallic domain size and the device-size-dependent MIT property of VO₂ thin films grown on hBN. We observed by temperature-dependent Raman spectroscopy and optical microscopy the emergence of the metallic domains and determined the metallic domain size in VO₂ thin films grown on hBN. The metallic domain size of the VO₂ thin films grown on hBN was determined to be ~500 nm on average in length and up to sub-micrometer scale. Electric transport measurements revealed that VO₂/hBN microwires exhibit multi-level step-like resistivity changes that change by one to two orders when the length and width are ~2 μm owing to the confined metallic domains in the micrometer scale. Our results open a way for VO₂ devices, showing a steep and large resistance change even in the micrometer scale.

Published under an exclusive license by AIP Publishing. <https://doi.org/10.1063/5.0072746>

Vanadium dioxide (VO₂) exhibits metal–insulator transition (MIT) with three orders of magnitude resistance change near room temperature (~340 K),^{1,2} and the growth of VO₂ thin films has been studied for application to various devices, such as field-effect transistors and bolometers.^{3–5} Single-crystal oxide substrates such as Al₂O₃ and TiO₂ have been commonly utilized to grow high-quality VO₂ thin films. VO₂ thin films grown on Al₂O₃(0001) substrates show MIT at approximately 340 K, similarly to a bulk crystal owing to the relaxed strain.^{6,7} On the other hand, VO₂ thin films grown on TiO₂(001) substrates are single-crystal epitaxial thin films that show MIT at 300 K with the compressive strain along the *c*-axis.⁸ Recently, Genchi *et al.* have reported the growth of VO₂ thin films on hexagonal boron nitride (hBN).⁹ hBN is a two-dimensional layered material, where van der Waals interactions play a role in connecting each layer. Two-dimensional layered materials can reduce the lattice strain caused by

weak van der Waals interactions when used as substrates, making the lattice mismatch negligible at the interface between thin films and substrates. With its chemical stability and insulating property,^{10,11} hBN is suitable for growing oxide thin films. Stacks of VO₂/hBN are transferable onto various materials, such as gold, paper, and glass.⁹ These characteristics make the stacks of VO₂/hBN applicable to Mott transistors, paper electronics, smart windows, and so forth.⁹ Importantly, a VO₂/hBN microwire even with the length of 41 μm and width of 37 μm exhibits three orders of magnitude resistance change.⁹ These characteristics also indicate the possibility of hBN as a universal substrate for growing various oxide thin films regardless of lattice structures and lattice constants through van der Waals interactions.

Despite these advantages of VO₂ thin films grown on hBN, the relationship between the metallic domain size and the

device-size-dependent electric transport property such as the order of magnitude of the step-like resistance changes has yet to be determined. Generally, the MIT property is governed by a spatial element called “metallic domain,” and the metallic domain size is dependent on the substrate. For example, the metallic domain of VO₂ thin films grown on Al₂O₃($\bar{1}012$) substrates is observed by scanning near-field infrared microscopy,¹² and the metallic domain size of VO₂ thin films grown on Al₂O₃(0001) substrates is reported to be 50–70 nm.¹³ To obtain multi-level step-like resistance changes, nanowires have been fabricated to reduce the number of metallic domains.¹³ On the other hand, VO₂ thin films on TiO₂ substrates have two types of metallic domains: microsized domains and nano-sized domains. The microsized metallic domains, whose sizes are restricted by cracks formed on the surface, are observable by optical microscopy.^{14,15} Thus, a single-step resistance change changing by two orders in microwires has been reported.¹⁶ The nano-sized metallic domains have been observed through Kelvin probe force microscopy,^{17,18} and they are regarded as the original element to induce MIT. Based on these backgrounds, it is important to determine the metallic domain size, and it is necessary that the device size is small, on the order of the metallic domain size to obtain a steep and large resistance change since it can be a critical factor for enhancing the performance of the device using the MIT of VO₂ thin films.

In this study, the temperature-dependent *in situ* observation of MIT in VO₂ thin films grown on hBN was conducted, and the metallic domain size was determined to be ~500 nm on average and up to sub-micrometer scale from optical microscopy images. Furthermore, the device-size-dependent MIT property of VO₂ thin films grown on hBN was investigated by electric transport measurements using microwires. The multi-level step-like resistance changes were prominently observed when the width and the length were small enough to be comparable to the metallic domain size, ~2 μm . Notably, the giant single-step resistivity change changing by two orders owing to the confined metallic domains was observed.

hBN flakes were mechanically exfoliated and transferred from bulk crystals synthesized by the method of Taniguchi and Watanabe¹⁹ onto SiO₂/Si substrates, and the flakes were annealed in an oxygen atmosphere to remove the adhesive residue. Pulsed laser deposition (PLD) was utilized to grow VO₂ thin films with sintered V₂O₅ as a target and an excimer laser (193 nm). The partial oxygen pressure was 0.95 Pa, and the substrate temperature was 723 K. The crystallinity of the VO₂ thin films grown on hBN was characterized by temperature-dependent Raman spectroscopy (Raman touch, Nano photon) with a solid-state laser (532 nm). The laser spot size was ~1 μm , and the grating was 1200 lines/mm. Temperature-dependent *in situ* Raman spectroscopy was conducted at 300, 342, and 380 K on a temperature-controllable stage to identify the metallic domains. Next, temperature-dependent optical microscopy images were obtained to determine the metallic domain size. The metallic domain size was defined as the full width at half maximum of fitting Gaussian curves in the line profile of the color contrast. The cover ratio of the metallic domains over the observed area was calculated by binarization of the optical microscopy images. For these experiments, two VO₂/hBN flakes were prepared as shown in Table I to determine the metallic domain size in different VO₂/hBN flakes.

For electric transport measurements, a pair of electrodes were deposited by photolithography and sputtering deposition on VO₂/hBN flakes, and subsequently, VO₂/hBN microwires were fabricated

TABLE I. Thicknesses of VO₂ and hBN.

| | VO ₂ | hBN |
|-----------|-----------------|--------|
| Flake (1) | 80 nm | 95 nm |
| Flake (2) | 80 nm | 360 nm |

by photolithography and reactive ion etching under a mixture of O₂ and sulfur hexafluoride gases. The temperature-dependent resistivity of VO₂/hBN microwires was measured in air ambient on a thermally conductive Peltier stage in 0.1 K steps at a ramping/cooling rate of 1.5 K/min. To obtain the device-size-dependent resistivity–temperature (*R–T*) curves, three microwires with different widths and lengths were prepared, as shown in Table II. The VO₂/hBN microwires were fabricated from VO₂/hBN flakes different from flakes (1) and (2), which were prepared under the same experimental condition. Note that the wire (2) was fabricated by etching wire (1) to reduce the width of the microwire.

Figure 1(a) shows the optical microscopy image of flake (1) on the SiO₂/Si substrate, confirming the homogeneous formation of the thin film. Figure 1(b) shows the Raman spectra of the VO₂ thin film grown on hBN at 300 and 380 K. Clear Raman peaks attributable to VO₂ of the insulating monoclinic M1 phase were observed at 193, 223, 391, and 615 cm⁻¹,^{20,21} in addition to the Raman peaks of Si at 520 cm⁻¹ (Ref. 22) (used for calibration) and hBN at 1367 cm⁻¹ (Ref. 23) at 300 K. On the other hand, the Raman peaks attributable to VO₂ of the M1 phase disappeared at 380 K, implying that the VO₂ thin film grown on hBN underwent MIT accompanied by the structural change from the M1 phase to the rutile phase.²¹ Figure 1(c) shows a magnified monochrome optical microscopy image of flake (1) at 342 K during MIT. In this image, an inhomogeneous geometry composed of a gray region and black dots whose size was on the order of hundreds of nanometers was observed. Figure 1(d) shows the Raman spectra of the VO₂ thin film grown on hBN at 342 K. In the gray region, the Raman peaks attributable to the M1 phase were observed. On the other hand, the Raman spectra at a black dot exhibited no Raman peaks attributable to the M1 phase, similarly observed for the VO₂ thin film at 380 K. In a minority, Raman peaks owing to the monoclinic M2 phase were observed at 200 and 642 cm⁻¹ (Ref. 21) in addition to the Raman peaks attributable to the M1 phase due to the growth of VO₂ along the energetically favorable [110] direction to hBN(001)⁹ although the M2 phase was not able to be optically distinguished by the color contrast (see Fig. S1 in the supplementary material). These results suggest that the gray region and the black dots correspond to the insulator phase and the metallic phase, respectively. To determine the metallic domain

TABLE II. Sizes of VO₂/hBN microwires.

| | Length (<i>L</i>) | Width (<i>W</i>) |
|----------|---------------------|--------------------|
| Wire (1) | 23.5 μm | 12.7 μm |
| Wire (2) | 23.5 μm | 2.6 μm |
| Wire (3) | 1.1 μm | 2.6 μm |

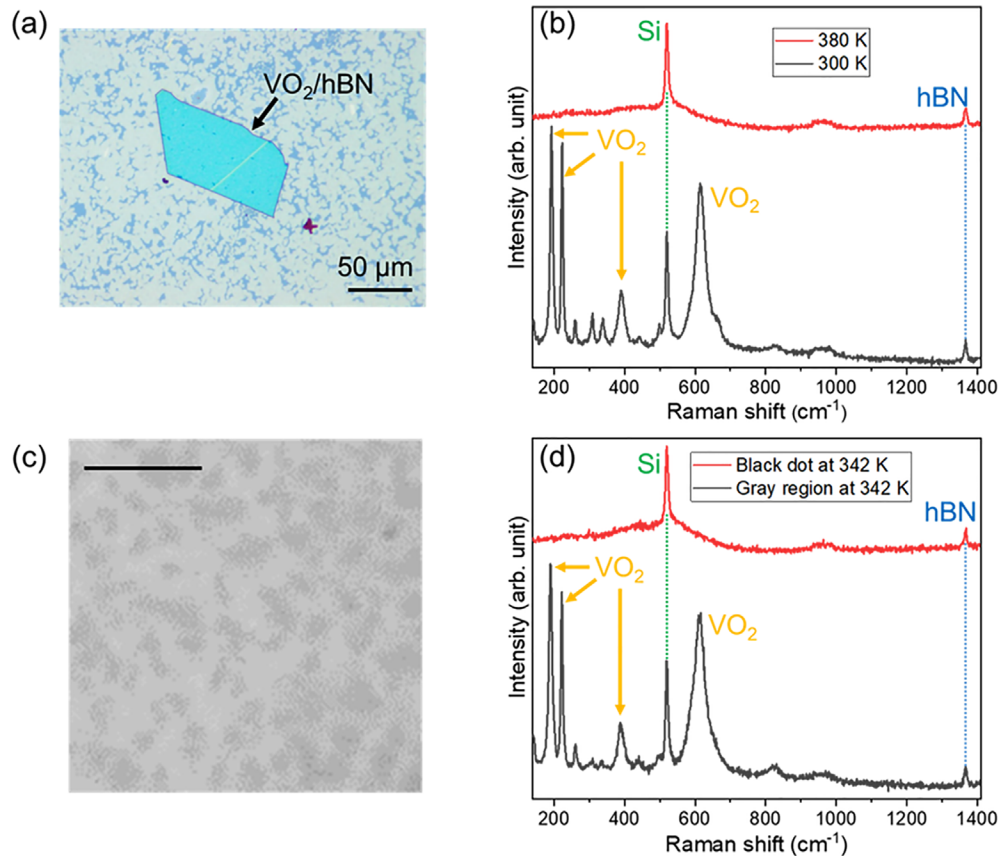


FIG. 1. (a) Optical microscopy image of flake (1). (b) Raman spectra of flake (1) at 300 and 380 K. The green and blue dotted lines correspond to the Raman peaks of Si and hBN, respectively. (c) Magnified monochrome optical microscopy image of flake (1) at 342 K composed of black dots and gray region. The scale bar is 5 μm . (d) Raman spectra of flake (1) at the gray region and a black dot at 342 K. The green and blue dotted lines correspond to the Raman peaks of Si and hBN, respectively.

size in the VO_2 thin films grown on hBN, temperature-dependent optical microscopy images were obtained.

Figure 2(a) shows the magnified temperature-dependent optical microscopy images of flake (1). Note that the images were obtained in the same region. Upon heating to 360 K, the metallic domains (corresponding to dark blue dots) appeared, and a clear change in the color contrast was observed. The color contrast was found to return to the initial one after cooling to 300 K. Figure 2(b) shows the temperature-dependent cover ratio of the metallic domains over the area of the optical microscopy images. Note that the cover ratio was defined to be 0% at 300 K and 100% at 360 K, since the entire area of the images was covered by the insulator and the metallic domains at each temperature. The temperature-dependent cover ratio exhibited hysteresis characteristics with a sharp increase above 340 K during the heating process. Figure 3(a) shows the magnified temperature-dependent optical microscopy images of the flakes (1) and (2) around 330 K, where the metallic domains start to appear. Note that the images were obtained in the same region in each flake. Figure 3(b) shows the temperature-dependent metallic domain size. In the narrow temperature range, it was found that the metallic domains appeared discretely, and the number of the metallic domains increased with the size of ~ 500 nm

on average in length, as shown in Fig. 3(b). Thus, the 500 nm-sized metallic domains are the spatial element in MIT. This mechanism is same as that of VO_2 thin films on $\text{Al}_2\text{O}_3(0001)$ substrates. Although the resolution of the optical microscopy was 100–350 nm, the metallic domains were observable and the metallic domain size was found to be ~ 500 nm on average and up to sub-micrometer scale, which is one order of magnitude larger than that of the VO_2 thin film grown on the $\text{Al}_2\text{O}_3(0001)$ substrate.¹³ It is considered that the metallic domains exist within the grains considering the crystallography. These results suggest that the multi-level step-like resistance changes can be observed even in micrometer scale owing to the confined metallic domains.

Figure 4(a) shows the R - T curves measured ten times consecutively for wire (1), exhibiting three orders of magnitude resistivity change at approximately 340 K in each measurement. The observed MIT property is consistent with the result of the increase in the cover ratio of the metallic domains shown in Fig. 2(b). Wire (1) was etched to fabricate wire (2) to reduce the width, as shown in the inset of Fig. 4(b). Figure 4(b) shows the R - T curves measured ten times consecutively for wire (2), exhibiting different multi-level step-like resistivity changes in each measurement. The electric conduction is governed

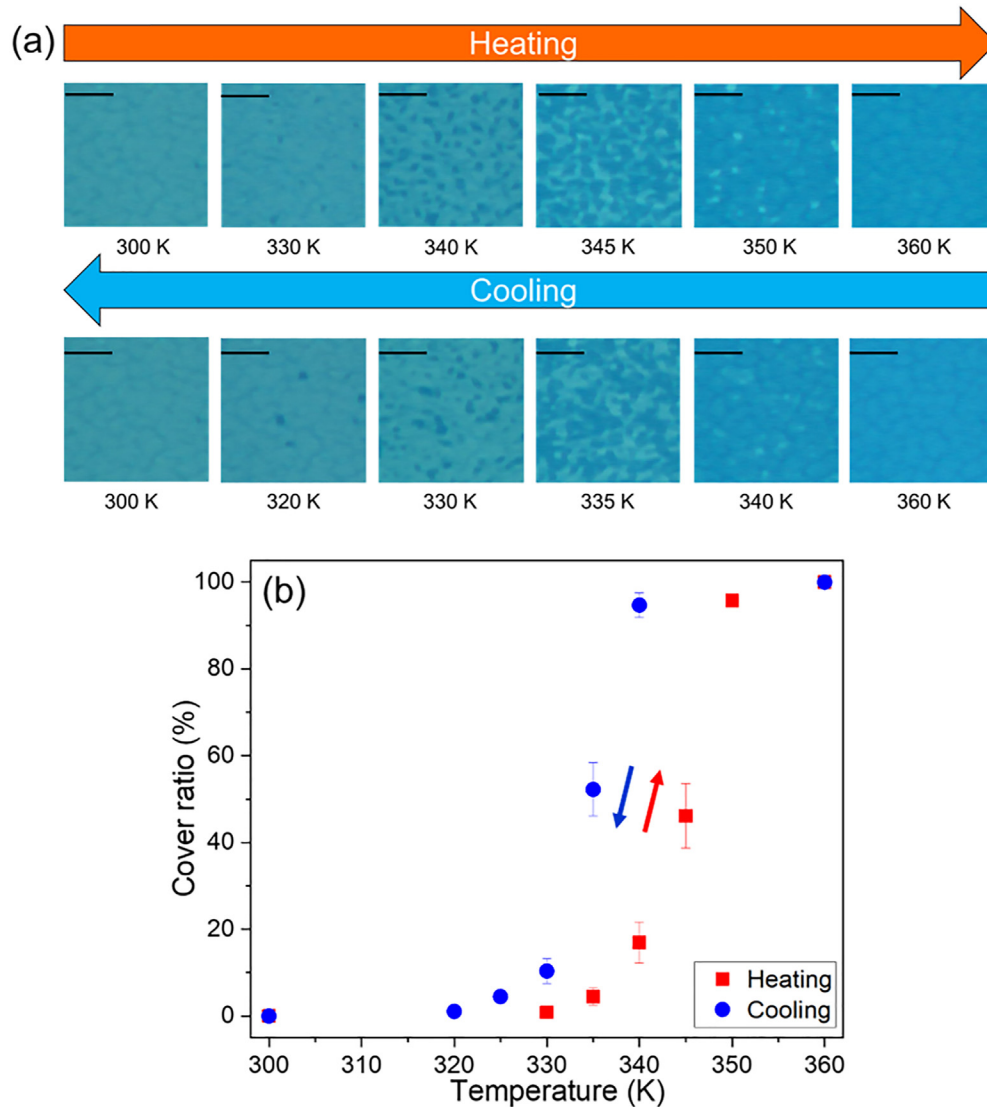


FIG. 2. (a) Magnified temperature-dependent optical microscopy images of flake (1) in the same region. The scale bars are 5 μm . (b) Temperature-dependent cover ratio of metallic domains. The red and blue curves correspond to the heating and cooling processes, respectively.

by the percolation paths,²⁴ and it has been estimated by a theoretical simulation that when the size of the microwire is several times larger than the metallic domain size, such multi-level step-like resistance changes appear owing to the confinement effect of the metallic domains.²⁵ Moreover, a similar electric behavior was also reported for the R - T curves measured eight times consecutively for a $\text{VO}_2/r\text{-Al}_2\text{O}_3$ device.²⁶ Figure 4(c) shows the schematic of the electric conduction path in the heating process between a pair of electrodes. The possible reason for such electric behavior is the fluctuation of the transition temperature of each metallic domain, leading to different electric conduction paths. However, the order of the resistivity/resistance change is considerably different. An approximately one order of magnitude resistivity change was observed in wire (2), whereas less than one order

of magnitude resistance change has been observed in the $\text{VO}_2/r\text{-Al}_2\text{O}_3$ device.²⁶ This result reflects the difference in the metallic domain size between VO_2 thin films grown on hBN and those grown on Al_2O_3 .

Next, to enhance the confinement effect of the metallic domains, wire (3) was prepared as shown in the inset of Fig. 5. Figure 5 shows R - T curves measured ten times consecutively for wire (3). The frequency and order of magnitude of the multi-level step-like resistivity changes became more pronounced than those of wire (2), as shown in Fig. 4(b). For comparison, a $\text{VO}_2/\text{Al}_2\text{O}_3(0001)$ microwire with $L = 2.4 \mu\text{m}$ and $W = 2.3 \mu\text{m}$ was fabricated, and R - T curves were obtained under the same experimental conditions (see Fig. S2 in the supplementary material). In the $\text{VO}_2/\text{Al}_2\text{O}_3$ microwire, no multi-level step-like resistivity changes were observed despite the comparable

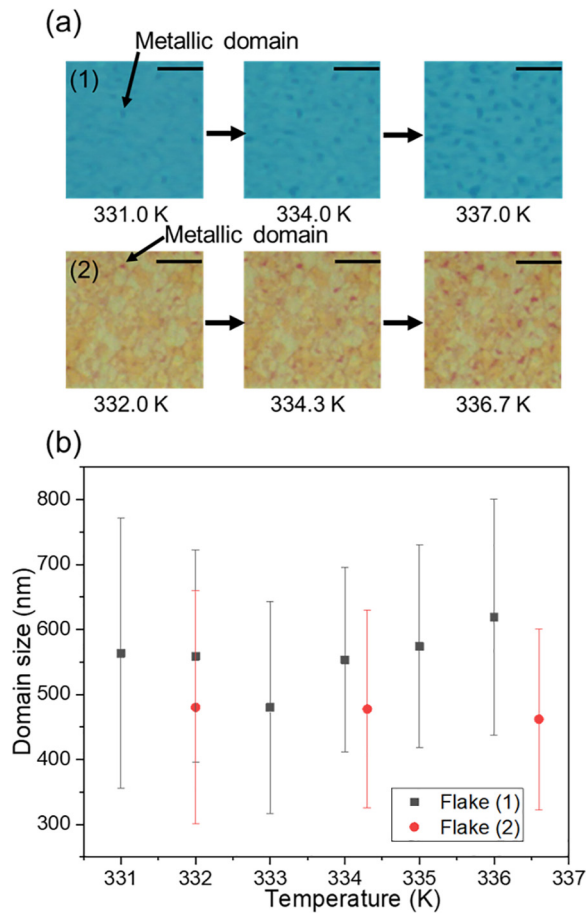


FIG. 3. (a) Magnified temperature-dependent optical microscopy images of flakes (1) and (2) in the same region in each flake. The metallic domains correspond to the dark blue and red dots in flakes (1) and (2). The scale bars are 5 μm . (b) Temperature dependence of the metallic domain size of flakes (1) and (2).

device sizes, which reflects the difference in the metallic domain size of $\text{VO}_2/\text{Al}_2\text{O}_3$ and VO_2/hBN . Furthermore, the giant single-step resistivity change changing by two orders was observed in wire (3), as shown in Fig. 5. Such giant single-step resistivity change is observed when the metallic domain size is comparable to the wire length.^{27,28} Considering that the length of wire (3) is 1.1 μm , the observed giant single-step resistivity change implies the presence of a metallic domain with the size comparable to 1.1 μm . This is reasonable since the optically determined metallic domain size was up to sub-micrometer scale. Therefore, the giant single-step resistivity change is attributable to the limited number of metallic domains in wire (3). It is also of great importance that such a giant single-step resistivity change was observed even in micrometer scale. Our results indicate the applicability of VO_2 thin films to switching devices, such as Mott transistors with the steep and large resistance change in micrometer scale.

In conclusion, the metallic domain size of VO_2 thin films grown on hBN is ~ 500 nm on average in length and up to sub-micrometer scale, as determined by temperature-dependent Raman spectroscopy and *in situ* optical observation. The multi-level step-like resistivity

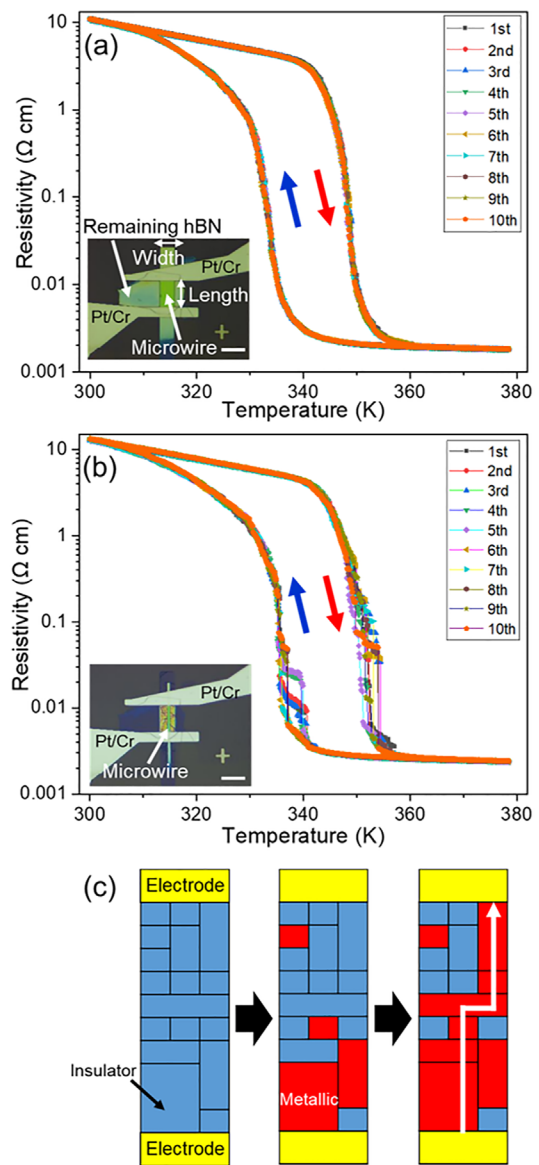


FIG. 4. (a) R - T curves measured ten times consecutively for wire (1). The inset is the optical microscopy image of wire (1). The thickness of the VO_2 thin film is 52 nm. The red and blue arrows indicate the heating and cooling processes, respectively. The scale bar is 20 μm . (b) R - T curves measured ten times consecutively for wire (2). The inset is the optical microscopy image of wire (2). The scale bar is 20 μm . (c) Schematic of the electric conduction path in the heating process between a pair of electrodes. The blue and red areas correspond to the insulator phase and metallic phase, respectively. The white arrow indicates the electric conduction path.

changes are attributed to the confinement effect in the micrometer scale. Importantly, the giant single-step resistivity change changing by two orders was observed, implying the presence of the metallic domain whose size is comparable to 1.1 μm . Our results show the usefulness of the application of VO_2/hBN to switching devices with a steep and large resistance change in the micrometer scale.

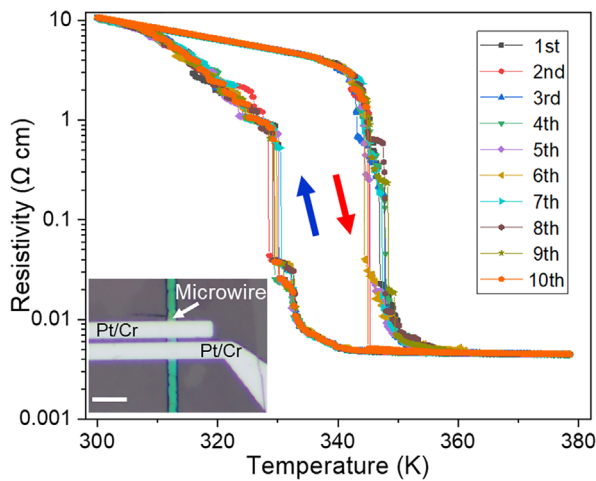


FIG. 5. R - T curves measured ten times consecutively for wire (3), showing the giant single-step resistivity change changing by two orders. The thickness of VO_2 is 50 nm. The inset is the optical microscopy image of wire (3). The scale bar is 10 μm .

See the [supplementary material](#) for the Raman spectrum of flake (1) with the Raman peaks attributable to the M2 phase at 342 K and R - T curves measured ten times consecutively for the $\text{VO}_2/\text{Al}_2\text{O}_3$ microwire.

We thank S. Sakakihara for etching the wires. This work was partly supported by a Grant-in-Aid for JSPS Fellows under Grant No. 20J21010, JSPS KAKENHI under Grant Nos. 19K15026 and 17H01054, The Murata Science Foundation, the Nippon Sheet Glass Foundation for Materials Science and Engineering, and Nanotechnology Open Facilities in Osaka University.

AUTHOR DECLARATIONS

Conflict of Interest

The authors have no conflicts to disclose.

DATA AVAILABILITY

The data that support the findings of this study are available within the article and its [supplementary material](#).

REFERENCES

- ¹F. J. Morin, *Phys. Rev. Lett.* **3**, 34 (1959).
- ²C. N. Berglund and H. J. Guggenheim, *Phys. Rev.* **185**, 1022 (1969).
- ³T. Yajima, T. Nishimura, and A. Toriumi, *Nat. Commun.* **6**, 10104 (2015).
- ⁴S. Sengupta, K. Wang, K. Liu, A. K. Bhat, S. Dhara, J. Wu, and M. M. Deshmukh, *Appl. Phys. Lett.* **99**, 062114 (2011).
- ⁵C. Chen, X. Yi, X. Zhao, and B. Xiong, *Sens. Actuators, A* **90**, 212 (2001).
- ⁶K. Okimura and J. Sakai, *Jpn. J. Appl. Phys., Part 1* **48**, 045504 (2009).
- ⁷J. Sang, T. Zheng, L. Xu, X. Zhou, S. Tian, J. Sun, X. Xu, J. Wang, S. Zhao, and Y. Liu, *J. Alloys Compd.* **876**, 160208 (2021).
- ⁸Y. Muraoka and Z. Hiroi, *Appl. Phys. Lett.* **80**, 583 (2002).
- ⁹S. Genchi, M. Yamamoto, K. Shigematsu, S. Aritomi, R. Nouchi, T. Kanki, K. Watanabe, T. Taniguchi, Y. Murakami, and H. Tanaka, *Sci. Rep.* **9**, 2857 (2019).
- ¹⁰A. G. F. Garcia, M. Neumann, F. Amet, J. R. Williams, K. Watanabe, T. Taniguchi, and D. Goldhaber-Gordon, *Nano Lett.* **12**, 4449 (2012).
- ¹¹G.-H. Lee, Y.-J. Yu, C. Lee, C. Dean, K. L. Shepard, P. Kim, and J. Hone, *Appl. Phys. Lett.* **99**, 243114 (2011).
- ¹²M. M. Qazilbash, M. Brehm, G. O. Andreev, A. Frenzel, P.-C. Ho, B.-G. Chae, B.-J. Kim, S. J. Yun, H.-T. Kim, A. V. Balatsky, O. G. Shpyrko, M. B. Maple, F. Keilmann, and D. N. Basov, *Phys. Rev. B* **79**, 075107 (2009).
- ¹³H. Takami, T. Kanki, and H. Tanaka, *Appl. Phys. Lett.* **104**, 023104 (2014).
- ¹⁴K. Kawatani, H. Takami, T. Kanki, and H. Tanaka, *Appl. Phys. Lett.* **100**, 173112 (2012).
- ¹⁵T. Kanki, K. Kawatani, H. Takami, and H. Tanaka, *Appl. Phys. Lett.* **101**, 243118 (2012).
- ¹⁶H. Ueda, T. Kanki, and H. Tanaka, *Appl. Phys. Lett.* **102**, 153106 (2013).
- ¹⁷A. Sohn, T. Kanki, K. Sakai, H. Tanaka, and D.-W. Kim, *Sci. Rep.* **5**, 10417 (2015).
- ¹⁸A. Sohn, T. Kanki, H. Tanaka, and D.-W. Kim, *Appl. Phys. Lett.* **107**, 171603 (2015).
- ¹⁹T. Taniguchi and K. Watanabe, *J. Cryst. Growth* **303**, 525 (2007).
- ²⁰M. Pan, J. Liu, H. Zhong, S. Wang, Z.-F. Li, X. Chen, and W. Lu, *J. Cryst. Growth* **268**, 178 (2004).
- ²¹K. Okimura, N. H. Azhan, T. Hajiri, S.-I. Kimura, M. Zaghrioui, and J. Sakai, *J. Appl. Phys.* **115**, 153501 (2014).
- ²²J. H. Parker, Jr., D. W. Feldman, and M. Ashkin, *Phys. Rev.* **155**, 712 (1967).
- ²³R. Geick, C. H. Perry, and G. Rupprecht, *Phys. Rev.* **146**, 543 (1966).
- ²⁴J. Rozen, R. Lopez, R. F. Haglund, Jr., and L. C. Feldman, *Appl. Phys. Lett.* **88**, 081902 (2006).
- ²⁵H. Tanaka, H. Takami, T. Kanki, A. N. Hattori, and K. Fujiwara, *Jpn. J. Appl. Phys., Part 1* **53**, 05FA10 (2014).
- ²⁶A. Sharoni, J. G. Ramirez, and I. K. Schuller, *Phys. Rev. Lett.* **101**, 026404 (2008).
- ²⁷Y. Tsuji, T. Kanki, Y. Murakami, and H. Tanaka, *Appl. Phys. Express* **12**, 025003 (2019).
- ²⁸S. Tsubota, A. N. Hattori, T. Nakamura, Y. Azuma, Y. Majima, and H. Tanaka, *Appl. Phys. Express* **10**, 115001 (2017).